CHAPTER 4

EFFECT OF ULTRASONIC SHOT PEENING ON ELECTROCHEMICAL CORROSION BEHAVIOR OF Ti–6Al–4V ALLOY

4.1 INTRDUCTION

Electrochemical tests were carried out for the USSPed of the specimens of alloy Ti–6Al–4V subjected to different peening durations of 0.25, 0.5, 1, 5, 10, 15 and 30 minute as well as the non-USSPed specimen in Ringer's solution, to examine the effect of surface nanostructure on corrosion behavior of this alloy. Some tests were carried out also following stress relieving treatment (SR) at 400 °C for 1h of the USSPed specimens. Surface morphology of the corroded samples was examined by SEM. The protective oxide layer was analysed through EDS. Corrosion resistance was improved from USSP, however, there was maximum improvement in corrosion resistance of the specimen USSPed for 1 minute. Corrosion resistance was reduced following SR treatment of the USSPed samples.

4.2 ELECTROCHEMICAL CORROSION

Electrochemical corrosion behavior of the non-USSPed, USSPed and USSPed+SR samples of the alloy Ti–6Al–4V was investigated in Ringer's solution by potentiodynamic polarization.

4.2.1   Corrosion Behavior

The typical potentiodynamic polarization curves for the non-USSPed and the differently USSPed specimens are shown in Fig. 4.1. It may be noted that for the specimen USSPed for 1 minute, corrosion potential shifted towards the more negative side. Passivation tendency may be seen to be highest for the USSPed 1 minute specimen in comparison to the others.
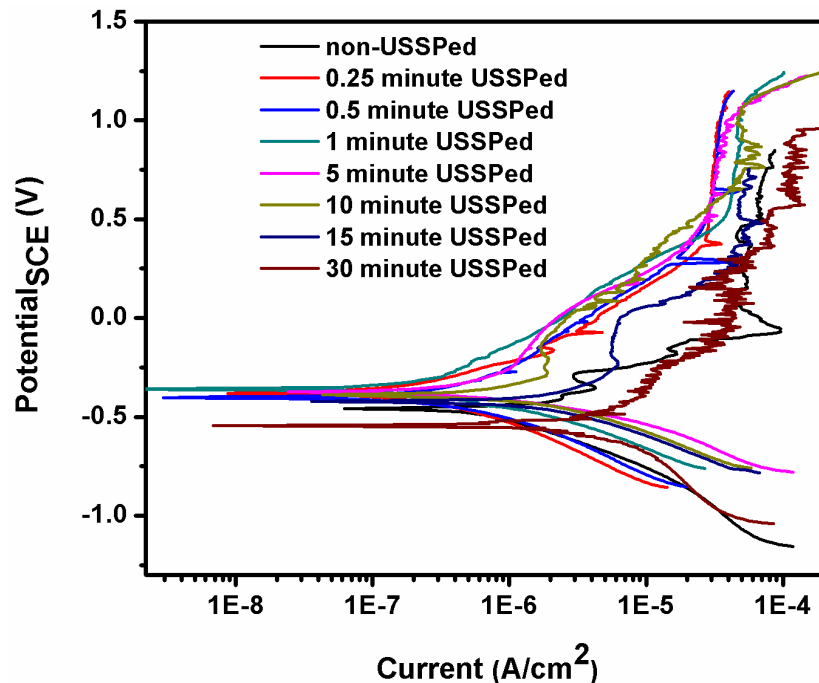
Fig. 4.1 Potentiodynamic polarization curves of the non-USSPed and USSPed 0.25, 1, 5, 15 and 30 minute in Ringer's solution.

Potentiodynamic polarization curves for the USSPed+SR samples are shown in Fig. 4.2. The USSPed, USSPed+SR and non-USSPed samples seem to exhibit apparent self-passivation. Corrosion resistance was reduced following SR treatment for the 1 and 5 minute USSPed specimens but was still higher than that of the non-USSPed specimen (Fig. 4.2).
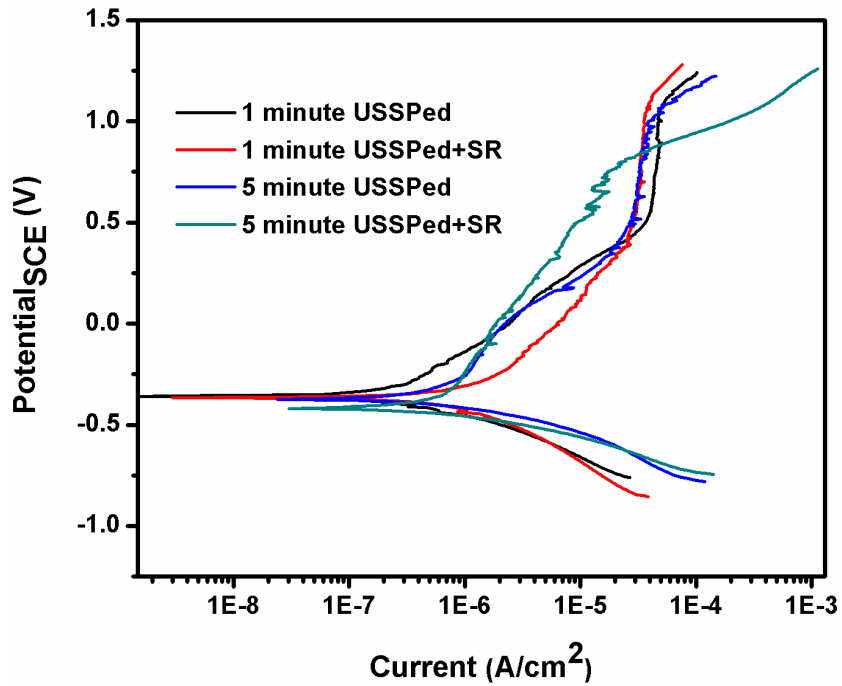
Fig. 4.2 Potentiodynamic polarization curves of the USSPed and USSPed+SR specimens in Ringer's solution.

The corrosion current density (i_{corr}), corrosion potential (E_{corr}), and corrosion rate of the each specimen was determined from the respective polarization curve. Corrosion rate was determined using the following equation [Ailor (1973)].

$$Corrosion\ rate\ (mpy) = 0.13 \times i_{corr} \times EW/d \ldots\ldots\ldots\ldots (4.1)$$

where mpy is corrosion rate expressed as mils per year, *EW* is equivalent weight, *d* is density (g/cm^3) of the alloy, and i_{corr} is corrosion current density ($\mu A/cm^2$), obtained by Tafel slopes (*βa and βc*). The corrosion parameters are presented in Table 4.1 and the variation of corrosion rate with the duration of USSP is shown in Fig. 4.3. It is well established that there is inverse relationship between corrosion current density and corrosion resistance. It was found that i_{corr} was drastically reduced for the USSPed 0.25 minute specimen and it was lowest for the USSPed 1 minute specimen. The current density was observed to increase gradually with further increase in the duration

of USSP up to 15 minute and suddenly to a much higher level for the specimen USSPed for 30 minute. Thus, it is obvious that corrosion resistance improved from the USSP and was maximum for the specimen USSPed for 1 minute. However, corrosion resistance started decreasing with further increase in the duration of USSP, up to 15 minute, and was drastically reduced for the sample USSPed for 30 minute.

Table 4.1 Corrosion current density (i_{corr}) and corrosion potential (E_{corr}) of the specimens non-USSPed, USSPed and USSPed+SR.

USSP duration (minute)	i_{corr} ($\mu A/cm^2$)	E_{corr} $mV_{(SCE)}$	Corrosion rate (mpy)	βa (V/decade)	βc (V/decade)
0	1.600	-457	1.060	0.218	0.370
0.25	0.499	-425	0.330	0.450	0.274
0.5	0.477	-395	0.316	0.440	0.279
1	0.268	-324	0.177	0.317	0.196
5	0.490	-348	0.324	0.342	0.180
10	0.614	-377	0.406	0.466	0.226
15	1.480	-422	0.980	0.401	0.297
30	4.110	-546	2.723	0.566	0.308
1minute USSPed+SR	0.589	-369	0.390	0.442	0.192
5minute USSPed+SR	0.634	-412	0.420	0.472	0.318

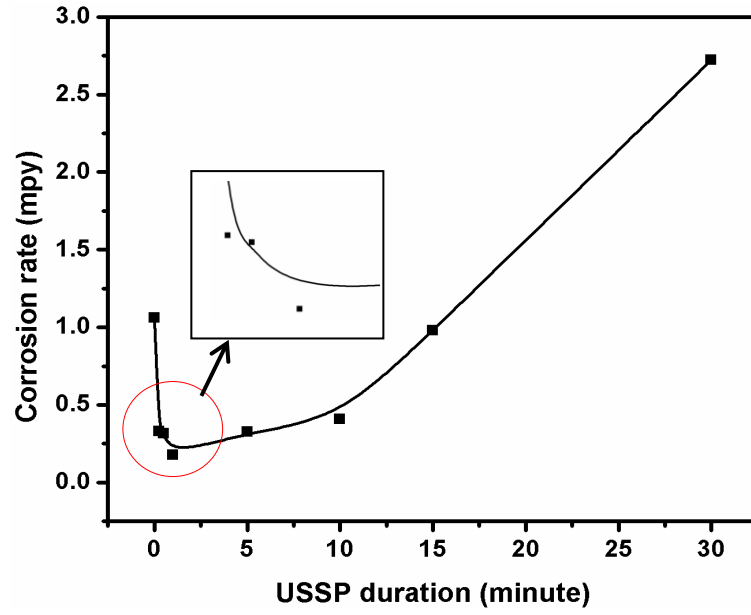βa = anodic Tafel slope
βc = cathodic Tafel slope

Fig. 4.3 Variation of corrosion rate with duration of USSP.

4.2.2 SEM and EDS Analysis

The surface morphology and EDS analysis of the corroded non-USSPed, USSPed and USSPed+SR specimens are shown in Figs. 4.4, 4.5 and 4.6 respectively. The EDS data pertain to the encircled region.
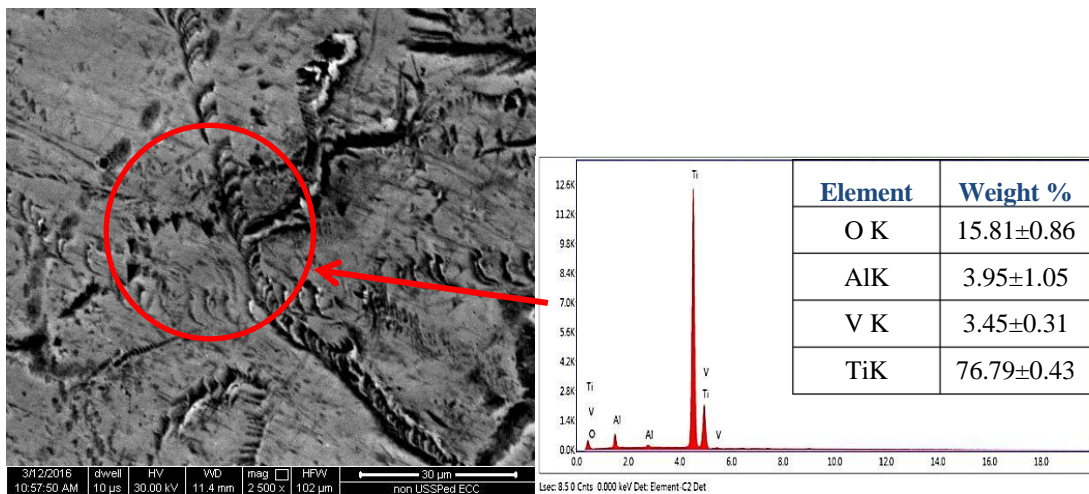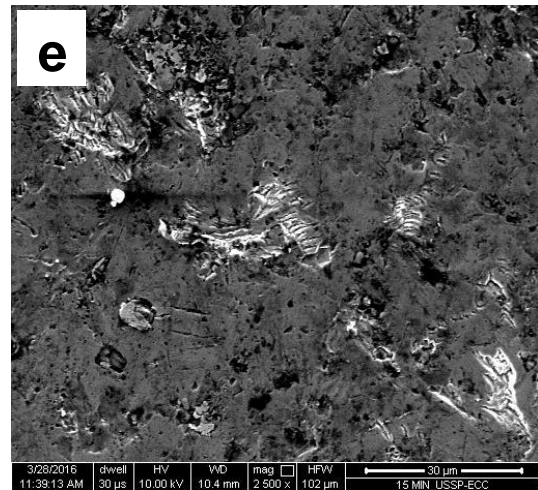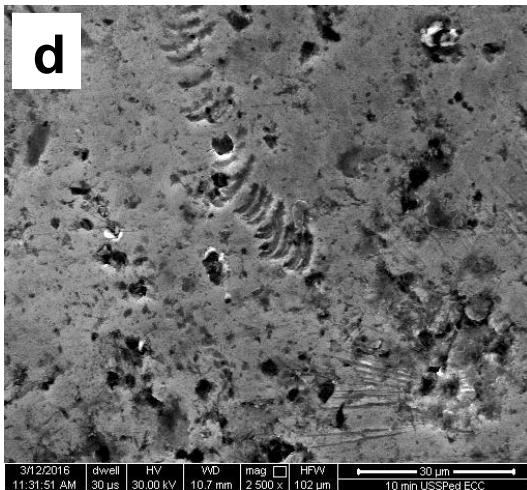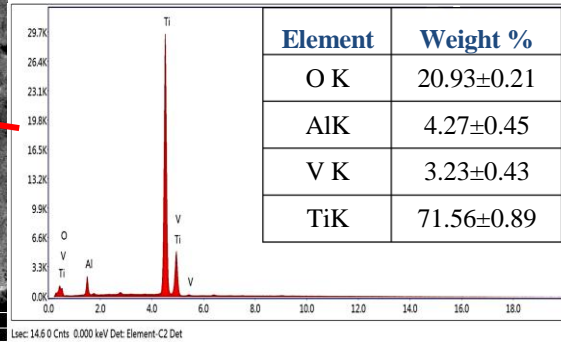

Element	Weight %
O K	15.81±0.86
AlK	3.95±1.05
V K	3.45±0.31
TiK	76.79±0.43

Fig. 4.4 Surface micrograph and EDS analysis of the corroded non-USSPed sample.

Element	Weight %
O K	20.93±0.21
AlK	4.27±0.45
V K	3.23±0.43
TiK	71.56±0.89

Element	Weight %
O K	23.09±0.26
AlK	4.07±0.08
V K	2.87±0.09
TiK	69.96±0.26
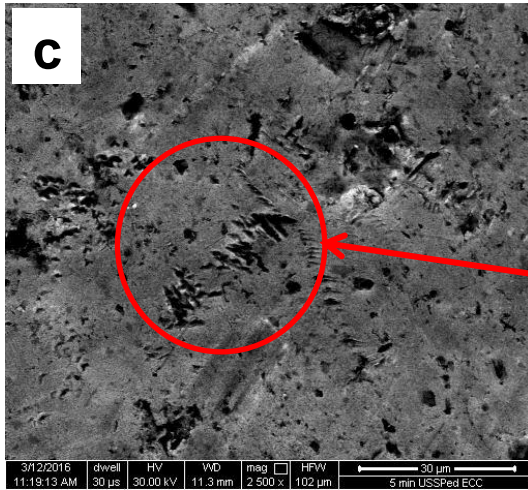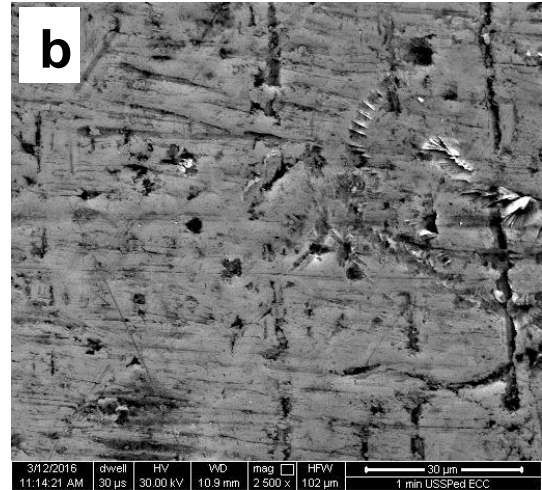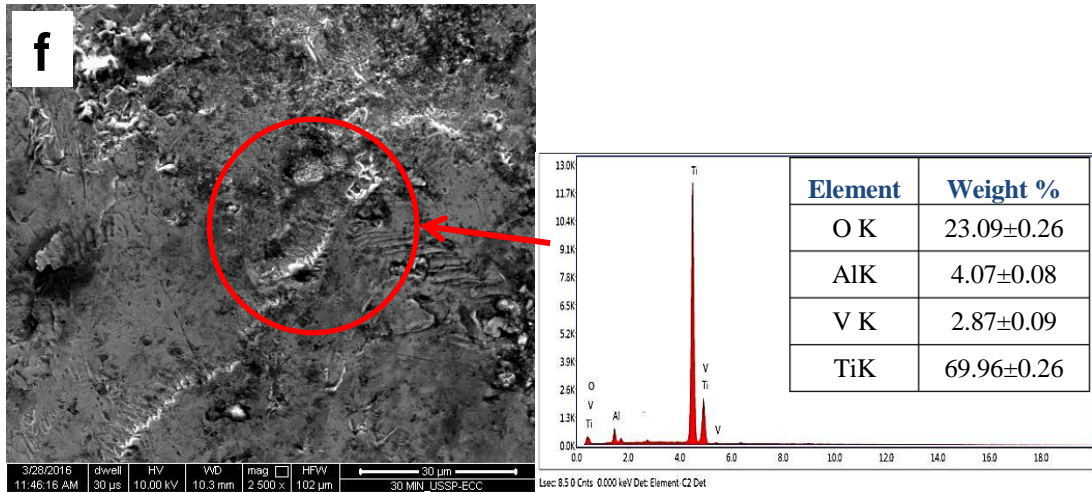
Fig. 4.5 Surface micrographs and EDS analysis of the corroded samples, USSPed for different durations: (a) 0.25 minute, (b) 1 minute, (c) 5 minute, (d) 10 minute, (e) 15 minute and (f) 30 minute.
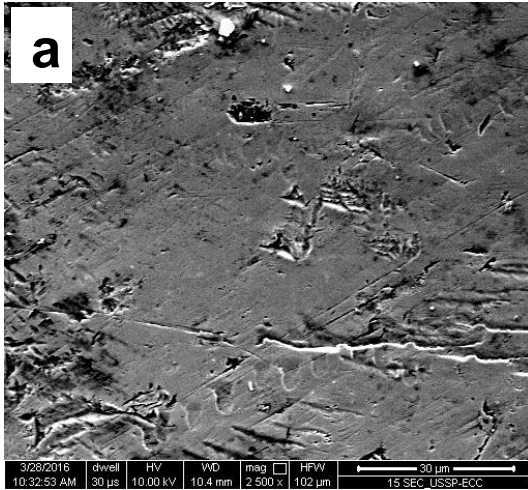

Element	Weight %
O K	19.75±0.17
AlK	5.07±0.12
V K	3.31±0.49
TiK	71.85±0.10
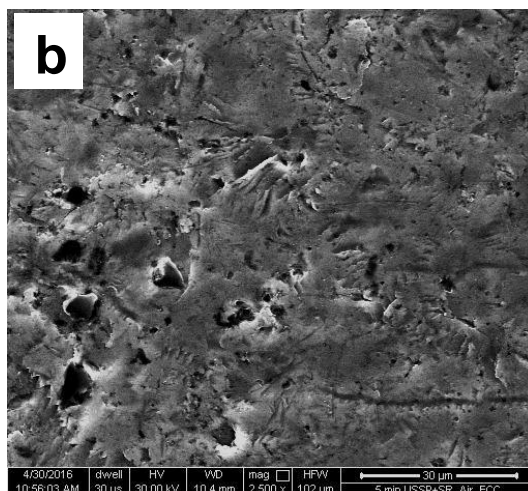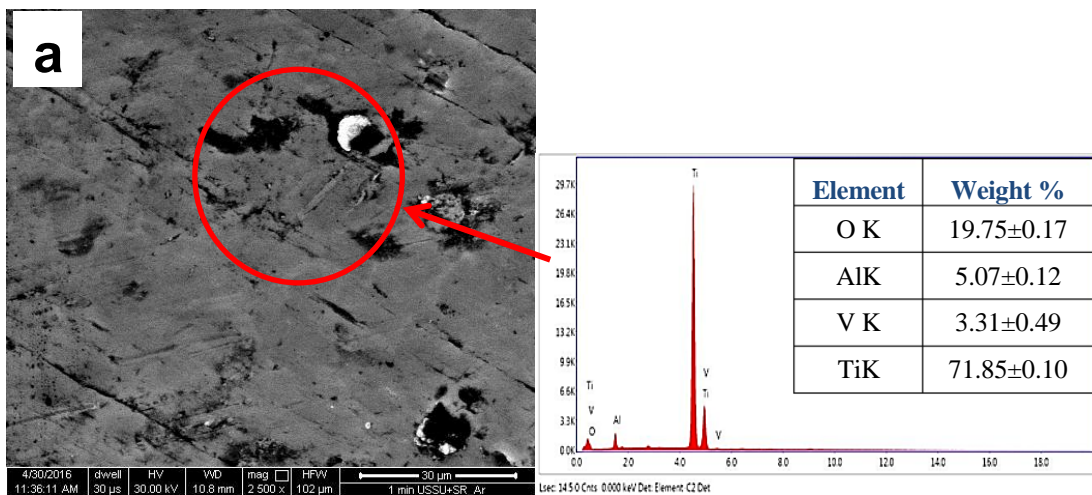
Fig. 4.6 Surface morphology of corroded specimens: (a) 1 minute USSPed+SR, and (b) 5 minute USSPed+SR.

SEM examination of the corroded samples showed higher degree of pits in the non-USSPed specimen in comparison to the specimens USSPed up to 15 minute and the USSPed+SR specimens. However, extensive pitting was observed in the USSPed 30 minute sample in comparison with the non-USSPed sample and also the size of the pits was larger than that of the other conditions. A similar trend may also be seen in the resistance against pitting in the above conditions. The pits of the USSPed+SR specimens were larger in size (Fig. 4.6) than those of the USSPed ones (Fig. 4.5b and 4.5c), corrosion resistance of the USSPed specimen was decreased after the SR treatment. It may also be noted that surface smoothness is deteriorated with shot peening duration.

EDS elemental analysis of the corroded surfaces was carried out and Ti, Al, V and O were detected. It was confirmed that various oxide products such as TiO_2, Al_2O_3, V_2O_3 and V_2O_5 were formed on the corroded surfaces. Balakrishnan et al. (2008) also reported corrosion products (TiO_2, Al_2O_3 and V_2O_3) in the nanocrystalline cp-Ti following potentiodynamic polarization.

4.3 DISCUSSION

As evident from the Table 4.1 corrosion current density was lowest for the USSPed 1 minute specimen and it exhibited the highest corrosion resistance among all the specimens subjected to USSP for different durations from 0.25 to 30 minute. Corrosion current density reflects the corrosion resistance [Okazaki et al. (1997)]. The lowest corrosion rate exhibited by the USSPed for 1 minute specimen may be attributed to rapid formation of a highly protective passive layer in this condition. It is obvious that grain refinement in the surface region to the level of nano scale played important role in enhancing the process of passivation. Formation of passive film depends on various

factors [Garbacz et al. (2007)]. Corrosion resistance of USSPed specimens have been correlated with grain size, lattice strain, dislocations and twins resulting from USSP [Huang et al. (2013), Li et al. (2004)].

It has been established from the studies on copper that increase in number density of grain boundaries enhanced the activity of electrons which resulted in decrease of the electron work function [Yu et al. (2005), Li (2006)]. In consequence, the surface became more electrochemically reactive and increased the passivation ability significantly resulting in formation of passive layer of high mechanical strength and increased stability.

However, excessive USSP results in damage of the shot peened surface due to excessive work hardening. Damage of the USSPed surface disrupts the continuity and uniformity of the nanostructure surface region and likewise also that of the associated compressive residual stress. Thus, the marked improvement in corrosion resistance of this alloy by USSP even for the short duration of 0.25 minute may be attributed to rapid development of highly protective passive film, as explained above. The effectiveness of the passive film increased with the duration of USSP and there was maximum for the USSPed 1 minute specimen (Fig. 4.1).

Along with the refinement of grains in the surface region resulting from USSP, there was also compressive residual stress in the affected region, known to enhance corrosion resistance [Jindal et al. (2014)]. The corrosion resistance was found to reduce following stress relieving treatment (Fig. 4.2). However, with further increase in the duration of USSP, protective efficiency of the passive layer was decreased, due to prior damage of the USSPed layer, resulting from excessive work hardening and hence the rate of corrosion increased up to 15 minutes of USSP. It may, however, be noted that

corrosion rate, even of the USSPed 15 minute specimen was lower than that of the non-USSPed one, in spite of its surface cracking. However, corrosion rate rapidly increased from long duration of 30 minute of USSP.

The observations made on the effect of USSP on corrosion behavior of the alloy Ti–6Al–4V are similar to those made in the AISI 409 stainless steel [Balusamy et al. (2010)]. It was observed that corrosion resistance of this steel was increased by USSP using 2 mm balls for 15, 30 and 45 minute and by 5 mm balls for 15 minute which caused surface nano crystallization and promoted the formation of protective passive film. On the other hand, SMAT using 8 mm balls for all the treatment time studied and with 5 mm balls for 30 and 45 minute decreased the corrosion resistance due to increase in micro-strain and defect density during these treatments. In a similar way, Kwok et al. (2006) observed that pitting resistance of the 316L stainless steel increased with decrease in grain size and consequently the corrosion resistance was increased. Laleh et al. (2011) observed that corrosion resistance of AZ91D magnesium alloy was better for shorter duration of peening than that for the longer duration of peening because of less roughness on the surface.

Grain refinement in surface region was observed to play important role in improving corrosion resistance of AZ91D magnesium alloy [Song et al. (2011)]. Jelliti et al. (2013) observed that corrosion resistance of Ti–6Al–4V alloy was improved with decrease in grain size.

It may be seen from Figs. 4.4 and 4.5 that pitting resistance was highest for the USSPed 1 minute sample. Pitting resistance was less for the specimens USSPed for 10 minute and further decreased for the specimen USSPed for 30 minute and was lowest for the non-USSPed one. Thus, there was a similar trend in pitting resistance of the

material as for the corrosion rate in the respective conditions. The highest rate of corrosion in the 30 minute USSPed condition may be attributed to highest extent of surface damage in the form of pits/cracks resulting from excessive work hardening in those regions [Okazaki et al. (1997), Wei et al. (2009), Lu et al. (2004)]. Figure 4.6 shows that pitting resistance was reduced following the SR treatment in respect of the as USSPed sample for 1 minute (Fig. 4.5a). Various oxide products of Ti, Al, V and O were confirmed through EDS analysis.

Thus, corrosion behavior of the surface nano crystallized specimen cannot be explained only in terms of grain refinement; other factors like dislocation density, deformation, micro-twinning, compressive residual stress, surface roughness and cracking should also be considered.

High dislocation density and micro-twins promote corrosion resistance of materials [Huang et al. (2013), Lu et al. (2006)]. High corrosion resistance of nano crystalline AISI 409 stainless steel induced by USSP has been attributed to be associated with compressive residual stress and high dislocation density in near surface region of the material [Balusamy et al. (2010)]. The improvement observed in corrosion resistance of the USSPed 1 minute specimen may thus be attributed to optimum condition of grain refinement resulting from USSP and rapid formation of highly protective and uniform passive layer along with uniformity in the associated compressive stress. On the other hand, localized damage of the surface USSPed for longer durations, from excessive work hardening, counteracts the beneficial effects of surface grain refinement forming rapid and protective layer and the associated compressive stress, with increase in the duration of USSP.

Surface roughness also plays an important role in formation of passive layer and on corrosion resistance of material [Azar et al. (2010)]. Generally, smooth surface offers better corrosion resistance in comparison to rough surface. As, discussed in the previous chapter surface roughness increases with peening duration. It is important to point out that passive layer formed on the surface should be stable and insoluble in the corrosive media to protect the base material. USSP for optimum duration improves the corrosion resistance.

4.4 CONCLUSIONS

The following conclusions may be drawn from this chapter on the effect of USSP on electrochemical corrosion of Ti–6Al–4V alloy.

1) Corrosion resistance of the alloy Ti–6Al–4V was found to be highest for the specimen USSPed for 1 minute due to rapid formation of a highly protective and uniform passive layer.

2) Nano structured surface promoted formation of a highly protective surface layer of titanium oxide.

3) Increase in the duration of USSP to 5 minute and above caused damage to the surface from excessive localised work-hardening and thereby corrosion resistance was reduced.

4) Localised damage of the surface from excessive USSP led to fall in corrosion resistance of this alloy in spite of the development of nanostructure in the surface region.